Mg^{2+} Coordination in Catalytic Sites of F_1-ATPase†

Joachim Weber, Sean T. Hammond, Susan Wilke-Mounts, and Alan E. Senior*

Department of Biochemistry and Biophysics, University of Rochester Medical Center, Box 712, Rochester, New York 14642

Received September 24, 1997; Revised Manuscript Received November 3, 1997⊗

ABSTRACT: Coordination of the Mg^{2+} ion in Mg-nucleotide substrates by amino acid residue side chains in the catalytic site of *Escherichia coli* F_1-ATPase was investigated. From the X-ray structure of the mitochondrial enzyme [Abrahams, J. P., Leslie, A. G. W., Lutter, R., and Walker, J. E. (1994) *Nature 370*, 621−628], it may be inferred that the hydroxyl of βThr-156 is a direct ligand of Mg^{2+}, whereas the carboxyls of βGlu-181, βGlu-185, and βAsp-242 might contribute via intervening water molecules. Elimination of each respective functional group by site-directed mutagenesis, followed by determination of Mg−nucleotide and uncomplexed nucleotide binding affinities using a tryptophan probe, showed that βThr-156, βGlu-185, and βAsp-242 are all involved in Mg^{2+} coordination, whereas βGlu-181 is not. A derived structural model for the octahedral coordination around the Mg^{2+} ion is presented. The results indicate that the ADP-containing site in the X-ray structure is the catalytic site of highest affinity. Correct Mg^{2+} coordination is required for catalytic activity at physiological rates. Elimination of any one of the Mg^{2+}-coordinating residues led to complete loss of Mg^{2+}-dependent nucleotide binding cooperativity of the catalytic sites.

ATP synthase (F_1F_o-ATPase) catalyzes synthesis of ATP from ADP and P_i, driven by a proton gradient, in the last step of oxidative phosphorylation. It is also used in bacteria to generate a proton gradient, using ATP hydrolysis as energy source. ATP synthesis and hydrolysis occur in nucleotide binding sites located on the F_1 sector. F_1 may be easily detached from the membrane-embedded F_o sector; it acts as an ATPase and is widely used as an experimental system to investigate the catalytic mechanism [for recent reviews, see Nakamoto (*1*) and Weber and Senior (*2*)]. F_1 contains a total of six nucleotide binding sites, three of which, located on the three β-subunits, participate in catalysis. These catalytic sites show strong positive catalytic cooperativity. If only one site is occupied by MgATP, hydrolysis and release of products are slow ["unisite catalysis"; see Penefsky and Cross (*3*) and Senior (*4*)]. To achieve rapid, physiological catalysis rates, all three catalytic sites must be filled ["multisite catalysis"; see Weber and Senior (*2*)].

Recent years have brought important advances toward understanding of the F_1-ATPase catalytic mechanism. One was the X-ray structure of the catalytic core of bovine mitochondrial F_1 (*5*). Another was the demonstration of rotation of the central γ-subunit within the $\alpha_3\beta_3$-subunit hexagon (*6*, *7*), supporting a sequential mechanism involving three catalytic sites (*2*, *8*). A third was the development of a true equilibrium technique for determination of nucleotide binding parameters of all three catalytic sites by site-directed tryptophan fluorescence (*9*, *10*). To analyze the mechanism of the enzyme at the molecular level it is now feasible to identify residues with a possible role in catalysis from the X-ray structure and then use site-directed mutagenesis in combination with the tryptophan fluorescence technique to determine the actual function of these residues.

The true substrates of ATP synthase are the Mg^{2+}−nucleotide complexes. There is a precise correlation between catalytic activity and catalytic site Mg^{2+}−nucleotide binding cooperativity. In absence of Mg^{2+} all three catalytic sites bind free ATP or ADP with the same low affinity and there is no catalysis. In the presence of Mg^{2+}, pronounced binding cooperativity among the three catalytic sites is observed (*11*). It is a basic tenet of all current models of the mechanism that only the one catalytic site which is in the "highest-affinity state" (which is formed only in presence of Mg^{2+}) is catalytically competent (*2*).

Given the central role that Mg^{2+} plays in catalysis, it is important to identify all the residues that contribute to coordination of the cation and to determine their function. In the X-ray structure (*5*), six residues come within 5.0 Å of Mg^{2+} in the MgAMPPNP-containing catalytic site, as follows: βThr-156[1] (shortest distance from Mg^{2+} is 2.3 Å to the hydroxyl oxygen); βGlu-181 (3.7 Å to a carboxyl oxygen); βAsp-242 (4.0 Å to a carboxyl oxygen); βArg-182 (4.0 Å to a guanidino nitrogen); βGlu-185 (4.1 Å to a carboxyl oxygen); and βLys-155 (4.7 Å to C_ϵ). In the MgADP-containing catalytic site, in addition to the six residues listed above, residue αArg-376 comes within 5.0 Å of the Mg^{2+} ion (4.8 Å to a guanidino nitrogen).

Mg^{2+} has a strong propensity to assume an octahedral coordination, and the average distance between Mg^{2+} and a coordinating oxygen is 2.1 Å (*12*). Thus, in F_1 catalytic sites the only residue that could directly contribute to the first coordination sphere is βThr-156, via its hydroxyl oxygen. In the MgAMPPNP-containing site, one oxygen atom from

† Supported by NIH Grant GM25349 to A.E.S.
⊗ Abstract published in *Advance ACS Abstracts,* December 15, 1997.

[1] Residue numbers refer to the *E. coli* enzyme.

S0006-2960(97)02370-2 CCC: $15.00
Published on Web 01/13/1998

each of the β- and γ-phosphates is a direct ligand of the Mg^{2+} ion; in the MgADP-containing site, one oxygen atom of the β-phosphate (*5*). The remaining ligands are presumably water molecules held in place by amino acid side chains. If coordination occurs via an intervening water molecule, the anticipated distance between Mg^{2+} ion and an oxygen of the second coordination sphere is approximately 4 Å. Thus, in principle, each of the three negatively charged residues found in the vicinity of the Mg^{2+} ion, namely, βGlu-181, βGlu-185, and βAsp-242, could function to hold a Mg^{2+}-liganding water molecule in place.

A further residue for which a role in Mg^{2+} coordination was suggested is αSer-347. The results of electron spin resonance experiments with chloroplast F_1 indicated that in one conformation of the catalytic site another hydroxyl ligand, in addition to βThr-156, might be present in the first coordination sphere of the metal ion; based on the crystal structure (*5*), αSer-347 appeared to be the most likely candidate (*13*).

In this paper we present a detailed analysis of the environment of the Mg^{2+} ion in the catalytic sites of *Escherichia coli* F_1. The approach used was to first generate mutations that removed potential Mg^{2+}-coordinating side chains within the catalytic site, then to combine each mutation with the βY331W mutation (*9*) and use the fluorescence of the βTrp-331 residue to determine Mg^{2+}−nucleotide and free nucleotide binding affinities at each of the three catalytic sites. The results lead to a structural model of the octahedral coordination of Mg^{2+} in the catalytic site, involving residues βThr-156, βGlu-185, and βAsp-242, along with oxygen atoms of nucleotide phosphates.

EXPERIMENTAL PROCEDURES

E. coli Mutant Strains. Site-directed mutagenesis was performed by the method of Vandeyar et al. (*14*) using the T7-GEN mutagenesis kit (USB). To generate the βT156A/βY331W and βE185Q/βY331W mutations, the template was M13mp18 containing the *Hin*dIII−*Kpn*I fragment from plasmid pSWM4 (*9*), which contains the entire β subunit gene with the βY331W mutation. The mutagenic oligonucleotides were (i) GTGTAGGTAAA*GC*A*G*TT*A*ACAT-GAT, where the italicized base changes convert residue β156 from T to A (ACC to GCA) and introduce a *Hpa*I site; and (ii) GGTGAACGTAC*G*CGTCAGGGTAAC, where the italicized base changes convert residue β185 from E to Q (GAG to CAG) and introduce an *Mlu*I site. Phage replicative forms containing the desired mutations were identified by screening with the respective restriction enzyme. The mutations were transferred on an *Nhe*I−*Kpn*I fragment into pSWM4, generating the new plasmids pSTH1 (βT156A/βY331W) and pSTH3 (βE185Q/βY331W). The absence of any unwanted mutation was confirmed by sequencing of the entire β subunit gene. The plasmids were transformed into strain JP17 (*15*) to give strains STH1 (βT156A/βY331W) and STH3 (βE185Q/βY331W). To generate the αS347A mutation, the template was M13mp18 containing the *Sph*I−*Sal*I insert from plasmid pDP34 (*16*), which contains base pairs 3−1420 of the α subunit gene. The mutagenic oligonucleotide was CCAACG-TAATC*GC*G*A*TTACCGA, where the italicized base changes convert residue α347 from S to A (TCC to GCG) and introduce an *Nru*I site. Phage replicative forms containing the desired mutation were identified by screening with *Nru*I. The mutation was transferred on an *Xho*I−*Csp*45I fragment into plasmid pDP34N (*9*), generating the new plasmid pSWM67. The plasmid was transformed into strain AN888 (*17*) to give the new strain SWM67. Strains SWM32 (βE181Q/βY331W) and SWM36 (βD242N/βY331W) were as in Löbau et al. (*18*).

Enzyme Purification and Characterization. βT156A/βY331W, βE185Q/βY331W, βE181Q/βY331W, βD242N/βY331W, βY331W, and wild-type F_1 were prepared according to Weber et al. (*19*) from strains STH1, STH3, SWM32, SWM36, SWM4, and SWM1, respectively (*8*, *18*, *20*; this study). STH3 F_1 was further purified by a second gel-filtration chromatography at 23 °C (Sephacryl S300, 2.5 × 90 cm; buffer was 50 mM Tris/H_2SO_4, 40 mM Na_2SO_4, 2 mM $MgCl_2$, 1 mM ATP, 1 mM dithiothreitol, and 40 mM 6-aminohexanoic acid, pH 7.0). Purity and subunit composition of the F_1 preparations was checked by SDS−polyacrylamide gel electrophoresis (*21*). Protein concentrations of F_1 solutions were determined using the Bio-Rad protein assay (*22*).

Assays of Enzyme Function. Growth yield analyses in limiting (3 mM) glucose and tests of growth on solid succinate medium were performed as described (*23*). Standard ATPase activities were assayed in 50 mM Tris/H_2SO_4, 10 mM ATP, and 4 mM $MgSO_4$, pH 8.5, at 30 °C. Released P_i was determined by colorimetric assays (*24*, *25*).

Tryptophan Fluorescence Measurements. Nucleotide binding was measured by the quenching of βTrp-331 fluorescence. The experiments were carried out at 23 °C in spectrofluorometers type Spex Fluorolog 2 or Aminco Bowman 2. The excitation wavelength was 295 nm; the emission wavelength, 360 nm. Before use, the enzyme was preequilibrated in 50 mM Tris/H_2SO_4, pH 8.0, by consecutive passage through two 1 mL Sephadex G-50 centrifuge columns. In the experiments the same buffer was used, with either 2.5 mM $MgSO_4$ (MgATP and MgADP titrations) or 0.5 mM EDTA (free ATP and ADP titrations). F_1 concentration in the cuvette was 100−200 nM. Background signals (buffer) were subtracted; inner filter and volume effects were corrected for by performing parallel titrations with wild-type F_1. With MgATP as ligand, maximally two data points were acquired in a single experiment, to avoid interference by hydrolysis product MgADP. Binding parameters were determined by fitting theoretical curves to the measured data points; the binding models used are given in the text and in figure legends.

RESULTS

Functional Effects of the Mutations βT156A/βY331W, βE185Q/βY331W, and αS347A in Cells. Growth characteristics of the new mutant strains STH1 (βT156A/βY331W) and STH3 (βE185Q/βY331W) were tested and it was found that neither strain grew on succinate plates and that growth yields in liquid medium containing limiting glucose were the same as that of the Unc^- control (pUC118/JP17). These results corroborate previous findings obtained with the single mutants βT156A and βE185Q (*26*, *27*) and demonstrate that these mutations abolish ATP synthase activity *in vivo*. The mutation βY331W alone has only a minor effect on ATP synthase *in vivo* (*9*).

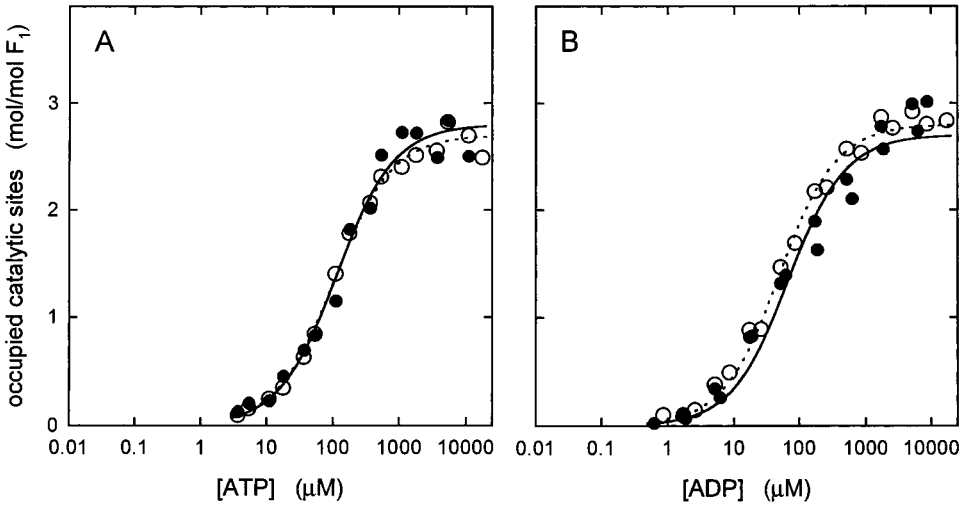

FIGURE 1: 1. Nucleotide binding to βT156A/βY331W mutant F_1. (A) ATP; (B) ADP. (●) Binding in the presence of 2.5 mM Mg^{2+}; (○) binding in the absence of Mg^{2+} and the presence of 0.5 mM EDTA. The lines are fits of theoretical curves to the experimental data points based on a binding model with *N* identical sites. Solid lines, fit to the data obtained in the presence of Mg^{2+}; dotted lines, fit to the data obtained in the absence of Mg^{2+} and the presence of EDTA.

The new mutant strain SWM67 (αS347A) grew well on succinate plates, and the growth yield in limiting glucose was identical to that of the wild-type control. Thus, the hydroxyl group of αSer-347 appeared to be of no functional importance, and the αS347A mutant was not further pursued.

Properties of Purified F_1 from the βT156A/βY331W and βE185Q/βY331W Mutant Strains. As judged from the Sephacryl S300 elution profile in the final purification step, and from SDS−polyacrylamide gel electrophoresis, purified F_1 from both double mutants showed the same molecular size and subunit composition as wild-type F_1. Yield of both preparations was low (0.04−0.08 mg of F_1/g wet weight of cells). The specific ATPase activity of βT156A/βY331W mutant F_1 was 0.017 unit/mg (0.1% of βY331W and 0.04% of wild-type F_1), and that of βE185Q/βY331W F_1 was 0.12 unit/mg (0.9% of βY331W and 0.36% of wild-type F_1). The former value agrees with data for the single βT156A mutant (*26*), but the latter value is substantially higher than that given for the single βE185Q mutant (*27*). However, several experiments demonstrated that the activity observed here is referable to true catalysis by βE185Q/βY331W mutant F_1. (1) pH dependence of the ATPase activity was the same as for βY331W and wild-type F_1. (2) ATPase activity was strongly inhibited by 10 μM aurovertin or 1 mM NaN_3. (3) It was confirmed that at the stage of harvesting of cells from the fermenter, no revertant (Suc^+) cells were present.

Tryptophan Fluorescence Properties of the Mutant Enzymes. The shape of the tryptophan fluorescence spectra of βT156A/βY331W and βE185Q/βY331W mutant F_1 was similar to that of βY331W F_1 [for examples see Figures 2 and 3 in Weber et al. (*9*)]. Upon addition of a saturating concentration of MgATP or MgADP, the fluorescence was substantially quenched. This is due to direct interaction between the adenine ring of the nucleotide and the βTrp-331 residue (*2*, *18*). Thus the effects of the βT156A and βE185Q mutations on nucleotide binding parameters can be monitored by following the βTrp-331 fluorescence.

Nucleotide Binding to βT156A/βY331W Mutant F_1. Figure 1A shows binding of MgATP and uncomplexed ("free") ATP to βT156A/βY331W mutant F_1. For comparison, Figure 2A shows parallel data for βY331W mutant F_1, which is representative of wild type. We should note that MgATP binding data shown in this study were obtained using a constant Mg^{2+} concentration of 2.5 mM. Previously (*9*, *11*, *18*) we had used a constant Mg^{2+}/ATP ratio of 4/10 in MgATP binding experiments. However, because mutants described here were found to have significant affinities for free nucleotide (see below) it was necessary to increase the Mg^{2+} concentration to avoid competition effects. It should be emphasized that this change in experimental setup had only minor effects on calculated MgATP binding parameters of βY331W F_1.

From Figures 1A and 2A it is evident that the mutation βT156A was responsible for prominent changes in the nucleotide binding pattern of the catalytic sites. The enzyme lost the pronounced Mg^{2+}-induced binding cooperativity that is so characteristic of binding of Mg^{2+}−nucleotide to normal, catalytically active F_1. Instead, all three catalytic sites bound MgATP with the same affinity. Also, the affinity for MgATP was not significantly different from that for free ATP. Thus the preference of the catalytic sites for Mg^{2+}−nucleotide over free nucleotide was lost. The calculated total number of binding sites, *N*, was 2.8 for MgATP and 2.7 for free ATP; K_d values are given in Table 1.

Figures 1B and 2B present data for binding of MgADP and free ADP to βT156A/βY331W and βY331W mutant F_1, respectively, leading to the same conclusions as above. The binding affinity for MgADP ($N = 2.7$) and free ADP ($N = 2.8$) was the same in the βT156A/βY331W mutant (calculated K_d values given in Table 1), and the normal Mg^{2+}-induced binding cooperativity was absent.

Nucleotide Binding to βE185Q/βY331W Mutant F_1. Figure 3 shows binding of MgATP, free ATP, MgADP, and free ADP to βE185Q/βY331W mutant F_1. Comparison with the data in Figure 2 (βY331W F_1) reveals the effects of the βE185Q mutation. βE185Q/βY331W mutant F_1 showed no significant preference for Mg-nucleotide over free nucleotide, and a model assuming a single class of binding site gave a

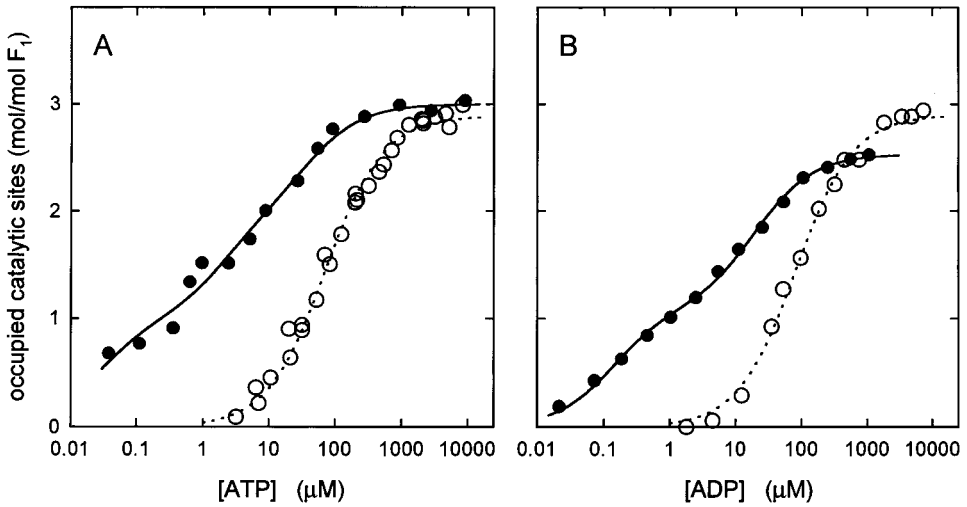

FIGURE 2: Nucleotide binding to βY331W mutant F_1. (A) ATP; (B) ADP. (●) Binding in the presence of 2.5 mM Mg^{2+}; (○) binding in the absence of Mg^{2+} and the presence of 0.5 mM EDTA. Solid lines, fit to the MgATP binding data (A), using a model with three sites of different affinities, or to the MgADP binding data (B), using a model with two classes of binding sites. Dotted lines, fit to the data obtained in the absence of Mg^{2+} and the presence of EDTA, based on a model with *N* identical binding sites. Binding data for MgADP, free ATP, and free ADP were taken from Weber et al. (*9*), Weber and Senior (*35*), and Löbau et al. (*18*), respectively.

Table 1: Catalytic Site Nucleotide Binding Parameters in Mutant Enzymes[a]

mutant	MgATP	free ATP	MgADP	free ADP
βY331W	$K_{d1} = 0.028$ $K_{d2} = 2.1$ $K_{d3} = 39$	$K_{d1,2,3} = 71$	$K_{d1} = 0.14$ $K_{d2,3} = 20$	$K_{d1,2,3} = 83$
βT156A/βY331W	$K_{d1,2,3} = 116$	$K_{d1,2,3} = 105$	$K_{d1,2,3} = 68$	$K_{d1,2,3} = 50$
βE185Q/βY331W	$K_{d1,2,3} = 2.0$	$K_{d1,2,3} = 3.5$	$K_{d1,2,3} = 6.5$	$K_{d1,2,3} = 3.2$
βD242N/βY331W	$K_{d1,2,3} = 17$	$K_{d1,2,3} = 20$	$K_{d1,2,3} = 19$	$K_{d1,2,3} = 11$
βE181Q/βY331W	$K_{d1} = 0.014$ $K_{d2} = 0.47$ $K_{d3} = 130$	$K_{d1,2,3} = 20$	$K_{d1} = 0.15$ $K_{d2,3} = 15$	$K_{d1,2,3} = 30$

[a] K_d values are given in micromolar.

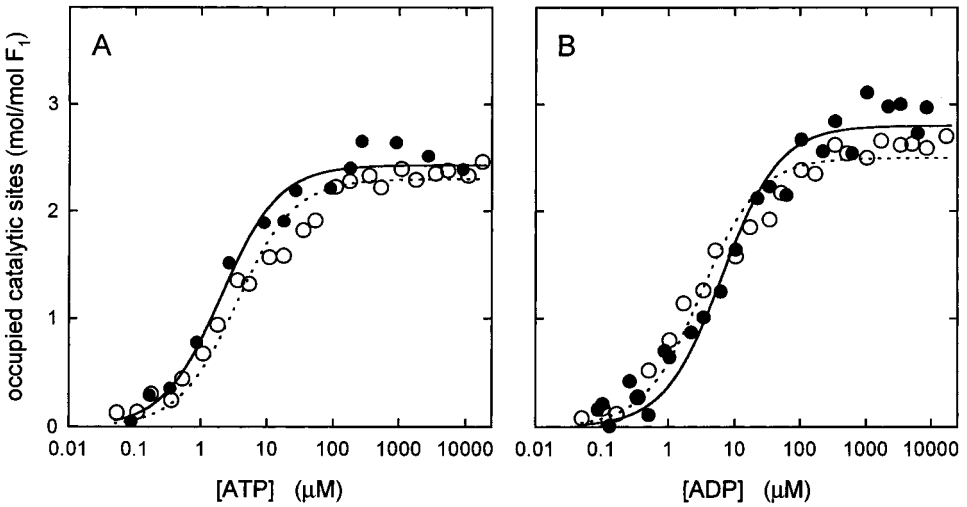

FIGURE 3: Nucleotide binding to βE185Q/βY331W mutant F_1. (A) ATP; (B) ADP. Symbols and binding models used are as in Figure 1.

satisfactory fit[2] for all nucleotides under investigation (N = 2.4 for MgATP, 2.3 for free ATP, 2.8 for MgADP, and 2.5 for free ADP; K_d values are given in Table 1). It is notable that βE185Q/βY331W mutant F_1 has clearly higher affinity for all four nucleotides tested than βT156A/βY331W F_1 and a satisfactory explanation is that removal of the negatively charged carboxyl group of residue β185 by the βE185Q mutation lessens electrostatic repulsion toward the nucleotide phosphates. Except for the generally higher affinity, the nucleotide binding pattern of βE185Q/βY331W is remarkably similar to that of βT156A/βY331W, and the data show conclusively that both residues βThr-156 and βGlu-185 are functionally critical for Mg^{2+} liganding in the catalytic site.

[2] We chose the simplest model that gave a satisfactory fit. In some cases where we used a model with a single class of binding sites, a model with nonidentical sites would have resulted in a slightly better fit, e.g., Figures 3A and 5. Thus we cannot rule out that in some of these cases the three catalytic sites have slightly different affinitites.

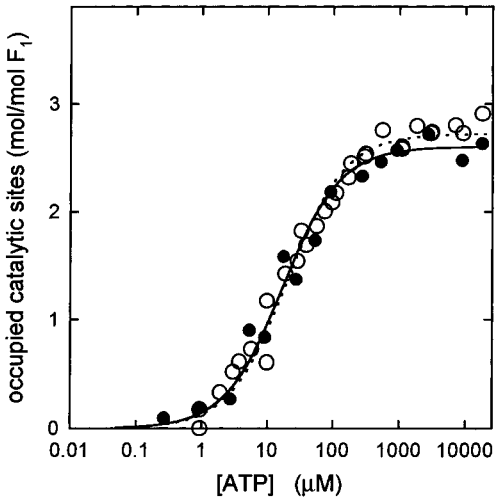

FIGURE 4: ATP binding to βD242N/βY331W mutant F_1. Symbols and binding models used are as in Figure 1. Data for binding of free ATP were taken from Löbau et al. (*18*).

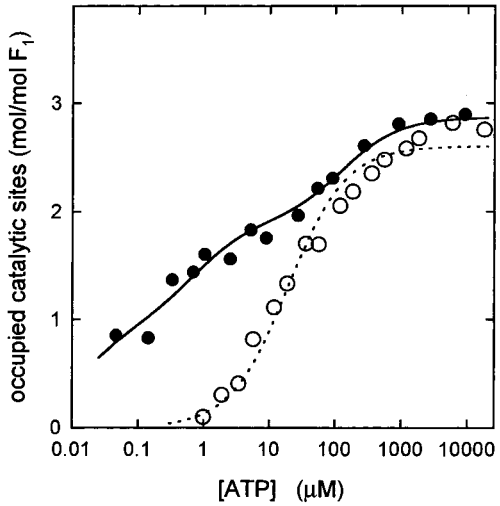

FIGURE 5: ATP binding to βE181Q/βY331W mutant F_1. Symbols and binding models used are as in Figure 2A. Binding data for free ATP were taken from Löbau et al. (*18*).

Nucleotide Binding to βD242N/βY331W and βE181Q/βY331W Mutant F1. In a recent study we described binding of nucleotides to catalytic sites of βD242N/βY331W mutant F_1 (*18*), establishing that residue βAsp-242 is functionally involved in Mg^{2+} liganding. The MgATP binding data in that report were obtained by titration with a solution containing $MgSO_4$ and ATP at a concentration ratio of 4/10 and were interpreted as showing some residual asymmetric (cooperative) binding behavior, although much less so than in catalytically active F_1. As noted above, as a result of data reported here it became apparent that since free ATP competes well with MgATP in some mutants where a Mg^{2+}-liganding side chain has been removed, a superior experimental approach is to use constant 2.5 mM Mg^{2+} concentration. The experiments shown in Figure 4 present such data for the βD242N/βY331W mutant F_1. It is seen that in the presence of 2.5 mM Mg^{2+} (●) as well as in its absence (○) all three catalytic sites exhibited the same affinity for ATP ($N = 2.6$, $K_d = 17$ μM for MgATP; $N = 2.7$, $K_d = 20$ μM for free ATP) with no evidence of residual asymmetry. Symmetric MgADP binding behavior of all three catalytic sites of βD242N/βY331W mutant F_1 was already reported in Löbau et al. (*18*) (see also Table 1). Thus, the new data show that the mutation βD242N leads to a nucleotide binding pattern resembling those caused by the mutations βT156A and βE185Q.

As described in the introduction, residue βGlu-181 is situated close to the bound nucleotide in the catalytic sites, but previous work had indicated that it is not directly involved involved in nucleotide binding (*18*). To further confirm this, we carried out experiments to measure binding of MgATP to βE181Q/βY331W mutant F_1 using a constant Mg^{2+} concentration of 2.5 mM. These data are shown in Figure 5. It is clear from comparison of Figures 1, 3, 4, and 5 that, in contrast to residues βThr-156, βGlu-185, and βAsp-242, the side chain of residue βGlu-181 is not necessary to preserve Mg^{2+}-induced nucleotide binding cooperativity. Rather, in βE181Q/βY331W mutant F_1 (Figure 5) as well as in catalytically normal βY331W F_1 (Figure 2), the presence of Mg^{2+} caused an asymmetric nucleotide binding pattern (see Table 1 for K_d values).

Effect of Excess Mg^{2+} on the ATPase Activity of βT156A/βY331W and βE185Q/βY331W Mutant F1. We previously demonstrated that whereas wild-type and βY331W F_1 exhibit pronounced inhibition of ATPase activity by excess Mg^{2+}, the mutation βD242N abolished this effect, confirming the role of residue βAsp-242 in Mg^{2+} binding (*18*). Determination of the ATPase activity of βT156A/βY331W and βE185Q/βY331W mutant F_1 as a function of increasing Mg^{2+} concentration at constant 5 mM ATP was carried out as described [see Figure 8 of Löbau et al. (*18*)] and resulted in a pattern very similar to that observed with βD242N/βY331W mutant enzyme. In all three cases, ATPase activity reached a maximum at approximately 5 mM Mg^{2+} and remained constant up to 25 mM Mg^{2+}. Thus the mutations βT156A and βE185Q abrogate inhibition by excess Mg^{2+}, confirming the involvement of these residues in Mg^{2+} complexation.

DISCUSSION

The goal of this study was to identify the amino acid residues that contribute to coordination of the Mg^{2+} ion in the catalytic nucleotide binding site of *Escherichia coli* F_1-ATPase. As described in the introduction, from the X-ray structure of mitochondrial F_1 (*5*) it may be inferred that the hydroxyl oxygen of βThr-156 is a candidate direct ligand of the Mg^{2+} ion and that the carboxyl groups of βGlu-181, βGlu-185, and βAsp-242 may coordinate Mg^{2+} via intervening hydrogen-bonded water molecules. Here we generated the mutations βT156A and βE185Q, combined each with the mutation βY331W, and used the fluorescence of residue βTrp-331 to measure the binding affinities of the three catalytic sites for MgATP, MgADP, free (i.e., uncomplexed) ATP, and free ADP. Also, we carried out further evaluation of the mutations βE181Q/βY331W and βD242N/βY331W, which had been constructed and described previously (*18*), and we briefly investigated the mutation αS347A.

On the basis of electron spin resonance experiments, Houseman et al. (*13*) had suggested that αSer-347 might be a direct ligand of the metal ion in the catalytic site. However, elimination of the hydroxyl group in αS347A mutant F_1 was without effect on oxidative phosphorylation *in vivo*. As

discussed below, correct coordination of the Mg^{2+} ion is critical to preserve the enzymatic activity; thus, it is highly unlikely that αSer-347 is involved in Mg^{2+} binding.

In contrast to αSer-347, the hydroxyl group of βThr-156 and the carboxyl groups of the three acidic residues βGlu-181, βGlu-185, and βAsp-242 are necessary to give a functional enzyme. Without these functional groups, oxidative phophorylation *in vivo* is blocked, and the ATPase activity of isolated F_1 is several orders of magnitude lower than normal (*26*−*32*; this study).

We found that, in regard to nucleotide binding behavior of the catalytic sites, three of the mutants under investigation were strikingly similar and very different from catalytically active enzyme. The three mutations, βT156A, βE185Q, and βD242N, each caused dramatic loss of Mg^{2+}-induced binding cooperativity. Preference for Mg^{2+}−nucleotide over free nucleotide was lost, and MgATP and MgADP bound to all three catalytic sites with the same affinity, just like free ATP and free ADP (Table 1). βT156A/βY331W mutant F_1 had an affinity for free ATP and ADP similar to that of βY331W F_1, while the affinity of βE185Q/βY331W and βD242N/βY331W mutant F_1 for free ATP and ADP was significantly increased (Table 1). These differences are most likely due to elimination of negative charge in the case of the carboxyl side chains, resulting in decreased repulsion of the negatively charged nucleotide phosphates. In contrast, F_1 from the fourth mutant, βE181Q/βY331W, displayed a nucleotide binding pattern that was similar to that of the active βY331W enzyme, with retention of Mg^{2+}-induced binding cooperativity, confirming that, as discussed previously, residue βGlu-181 is not directly involved in ligand binding (*18*, *29*, *31*).

The striking similarity of the effects of elimination of the functional groups of residues βThr-156, βGlu-185, and βAsp-242, i.e., loss of Mg^{2+}-induced cooperativity, loss of enzymatic function, and loss of inhibition of ATPase by excess Mg^{2+}, strongly suggests a common role for these three residues. The character of the functional effects, together with the X-ray structure information, leaves no doubt that this role is to provide coordination of the Mg^{2+} ion at the catalytic site. Because of its proximity, the hydroxyl group of βThr-156 certainly is a direct ligand of the metal ion, whereas βGlu-185 and βAsp-242, being more removed, must contribute to the coordination via an intervening hydrogen-bonded water molecule. Nevertheless, all three are functionally of similar importance.

Figure 6 shows a model for the coordination of the Mg^{2+} ion, based on the X-ray structure of the MgAMPPNP-containing catalytic site and the results of this study. The hydroxyl oxygen of βThr-156 and one oxygen atom each from the β- and γ-phosphates are in the same plane and occupy three of the six positions in the octahedron around the Mg^{2+} ion. Their planar configuration serves to define the equatorial plane of the octahedron in Figure 6. We have added three water molecules, designated A, B, and C, to complete the first coordination sphere. None of the water molecules resolved in the X-ray structure occupies any of these three positions.

The hypothetical water molecule A, in the apical position above the equatorial plane (Figure 6), can be easily accommodated by the X-ray structure. It is in the correct position for a water molecule hydrogen-bonded to the carboxyl group

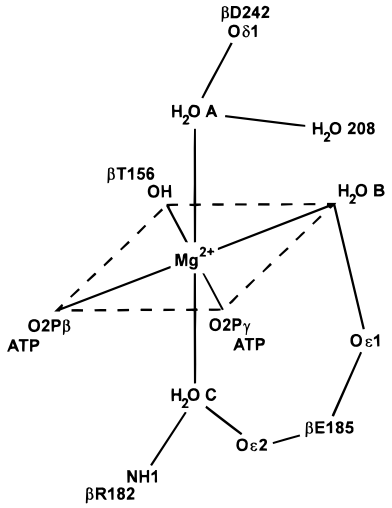

FIGURE 6: Model of Mg^{2+} coordination in the catalytic site of F_1. The model is based on the structure of the MgAMPPNP-containing catalytic site in the X-ray crystallography-derived model of mitochondrial F_1 (*5*) and on the results of the present study. Details are described in the text.

of residue βAsp-242; probably, it also interacts with a water molecule (H_2O 208) found in the X-ray structure. The two other hypothetical water molecules, one in the equatorial plane (B) and one in the other apical position (C), appear both to be hydrogen-bonded to the carboxyl group of residue βGlu-185. As the precise location of A, B, and C is not known, it is difficult to predict other ligands of these water molecules. The guanidino group of βArg-182 seems to be a possible ligand for C, and the amido group of βAsn-243 could be involved in coordination of A. The identification of further amino acid residues that participate in complexation of the Mg^{2+} ion via intervening water molecules A, B, and C will be the subject of future study.

One cannot discount the possibility that the Mg^{2+} ion has an incomplete first coordination sphere or that the coordination sphere is significantly distorted. In examples of other proteins that bind Mg^{2+}−nucleotide with high affinity, such as $p21^{ras}$ or myosin, it is seen that the ligands form a close-to-perfect octahedron around the Mg^{2+} ion (*33*, *34*). However, the X-ray structure of the MgAMPPNP-containing catalytic site in F_1 suggests that there is a certain amount of distortion of the first coordination sphere. If put into the perfect theoretical position, using the Mg^{2+} ion and the three planar nonwater ligands as reference, the hypothetical water molecule C comes rather close to the carboxyl oxygen Oϵ2 of residue βGlu-185, and more importantly, the van der Waals radius of the oxygen atom of water B would overlap with that of oxygen Oϵ1 of βGlu-181. In contrast, in the MgADP-containing catalytic site of F_1 (and in all three MgAMPPNP-containing noncatalytic sites) it is possible to introduce the hypothetical water molecules A, B, and C to form an undistorted octahedral first coordination sphere without interference with protein side chains. Given the functional importance of correct coordination of the Mg^{2+} ion, as demonstrated in the present study, the latter finding strongly supports the proposal made by Abrahams et al. (*5*) that in the X-ray structure the MgADP-filled site represents a catalytic site of higher affinity than the MgAMPPNP-containing site.

REFERENCES

1. Nakamoto, R. K. (1996) *J. Membr. Biol. 151*, 101−111.
2. Weber, J., and Senior, A. E. (1997) *Biochim. Biophys. Acta 1319*, 19−58.
3. Penefsky, H. S., and Cross, R. L. (1991) *Adv. Enzymol. Relat. Areas Mol. Biol. 64*, 173−214.
4. Senior, A. E. (1992) *J. Bioenerg. Biomembr. 24*, 479−484.
5. Abrahams, J. P., Leslie, A. G. W., Lutter, R., and Walker, J. E. (1994) *Nature 370*, 621−628.
6. Noji, H., Yasuda, R., Yoshida, M., and Kinosita, K., Jr. (1997) *Nature 386*, 299−302.
7. Yasuda, R., Noji, H., Kinosita, K., Jr., Motojima, F., and Yoshida, M. (1997) *J. Bioenerg. Biomembr. 29*, 207−209.
8. Boyer, P. D. (1989) *FASEB J. 3*, 2164−2178.
9. Weber, J., Wilke-Mounts, S., Lee, R. S. F., Grell, E. and Senior, A. E. (1993) *J. Biol. Chem. 268*, 20126−20133.
10. Weber, J., Bowman, C., and Senior, A. E. (1996) *J. Biol. Chem. 271*, 18711−18718.
11. Weber, J., Wilke-Mounts, S., and Senior, A. E. (1994) *J. Biol. Chem. 269*, 20462−20467.
12. Guerger, M. J., MacGillavry, C. H., Henry, N. F. M., Lonsdale, K., and Rieck, G. D. (1968) *International Tables for X-ray Crystallography*, pp 257−269, Kynoch Press, Birmingham, U.K.
13. Houseman, A. L. P., LoBrutto, R., and Frasch, W. D. (1995) *Biochemistry 34*, 3277−3285.
14. Vandeyar, M., Weiner, M., Hutton, C., and Batt, C. (1988) *Gene 65*, 129−133.
15. Lee, R. S. F., Pagan, J., Wilke-Mounts, S., and Senior, A. E. (1991) *Biochemistry 30*, 6842−6847.
16. Maggio, M. B., Parsonage, D., and Senior, A. E. (1988) *J. Biol. Chem. 263*, 4619−4623.
17. Downie, J. A., Cox, G. B., Langman, L., Ash, G., Becker, M., and Gibson, F. (1981) *J. Bacteriol. 145*, 200−210.
18. Löbau, S., Weber, J., Wilke-Mounts, S., and Senior, A. E. (1997) *J. Biol. Chem. 272*, 3648−3656.
19. Weber, J., Lee, R. S. F., Grell, E., Wise, J. G, and Senior, A. E. (1992) *J. Biol. Chem. 267*, 1712−1718.
20. Rao, R., Al-Shawi, M. K., and Senior, A. E. (1988) *J. Biol. Chem. 263*, 5569−5573.
21. Laemmli, U. K. (1970) *Nature 227*, 680−685.
22. Bradford, M. M. (1976) *Anal. Biochem. 72*, 248−254.
23. Senior, A. E., Latchney, L. R., Ferguson, A. M., and Wise, J. G. (1984) *Arch. Biochem. Biophys. 228*, 49−53.
24. Taussky, H. H., and Shorr, E. (1953) *J. Biol. Chem. 202*, 675−685.
25. van Veldhoven, P. P., and Mannaerts, G. P. (1987) *Anal. Biochem. 161*, 45−48.
26. Omote, H., Maeda, M., and Futai, M. (1992) *J. Biol. Chem. 267*, 20571−20576.
27. Omote, H., Le, N. P., Park, M. Y., Maeda, M., and Futai, M. (1995) *J. Biol. Chem. 270*, 25656−25660.
28. Yohda, M., Ohta, S., Hisabori, T., and Kagawa, Y. (1988) *Biochim. Biophys. Acta 933*, 156−164.
29. Senior, A. E., and Al-Shawi, M. K. (1992) *J. Biol. Chem. 267*, 21471−21478.
30. Park, M. Y., Omote, H., Maeda, M., and Futai, M. (1994) *J. Biochem. (Tokyo) 116*, 1139−1145.
31. Amano, T., Tozawa, K., Yoshida, M., and Murakami, H. (1994) *FEBS Lett. 348*, 93−98.
32. Amano, T., Hisabori, T., Muneyuki, E., and Yoshida, M. (1996) *J. Biol. Chem. 271*, 18128−18133.
33. John, J., Rensland, H., Schlichting, I., Vetter, I., Borasio, G. D., Goody, R. S., and Wittinghofer, A. (1993) *J. Biol. Chem. 268*, 923−929.
34. Fisher, A. J., Smith, C. A., Thoden, J. B., Smith, R., Sutoh, K., Holden, H. M., and Rayment, I. (1995) *Biochemistry 34*, 8960−8972.
35. Weber, J., and Senior, A. E. (1995) *J. Biol. Chem. 270*, 12653−12658.

BI972370E